

Guide to the Realization of the ITS-90

1 édition 2018

Partie 2.4

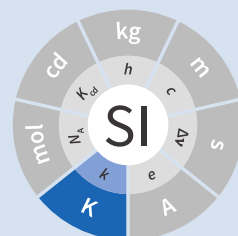
Part 2.4

Metal Fixed Points for Contact Thermometry

Consultative Committee for Thermometry

January 01, 2018

01 janvier 2018



**Guide to the Realization of the ITS-90
Part 2.4: Metal Fixed Points
for Contact Thermometry**

Consultative Committee for Thermometry

1st edition 2018

01 January 2018

Abstract

This paper is a part of guidelines, prepared on behalf of the Consultative Committee for Thermometry, on the methods for realizing the International Temperature Scale of 1990 (ITS-90).

It describes ways of realizing the defining fixed points of the ITS-90 which comprise metal fixed points for contact thermometry.

1. Introduction

This section describes ways of realizing the defining fixed points of the ITS-90 which comprise metals. A number of precautions must be taken if the highest accuracy is to be achieved. The defining fixed points of the ITS-90 concerned in this section are given in Table 1. Above the triple point of water, the assigned values of temperature are for equilibrium states at a pressure $p_0 = 101\,325\text{Pa}$ (one standard atmosphere). The gas pressure and hydrostatic pressure within fixed-point cells produce small but significant temperature effects, these are summarised in Table 1.

All metal fixed points must provide a continuous liquid-solid interface that, as nearly as is practical, encloses the sensing element of the thermometer being calibrated. As in the case of water triple point cells, for metal fixed points used for resistance thermometry two liquid-solid interfaces are generally induced. In such a situation, the outer interface advances slowly inward as the liquid continues to solidify (or the solid continues to liquefy). Ideally this generates a shell of uniform thickness completely surrounding the liquid (or the solid), which itself surrounds the inner liquid-solid interface that is adjacent to the thermometer well. The inner interface is essentially static except when heat is extracted, such as on the insertion of a cool replacement thermometer. It is the temperature of the inner liquid-solid interface which is measured by the thermometer. The equipment and the various techniques required in the generation of these interfaces, together with some methods of checking the quality of the results, are described below. Examples of achievable performance are given by [Strouse 2008]. For all fixed points, it is advisable to associate a so-called check-thermometer to monitor for unusual behaviour of the fixed point and test for the existence of the phase transition. The first part, *Guide Section 2.1 Influence of Impurities*, of *Guide Chapter 2 Fixed Points*, provides a detailed discussion of the determination of the liquidus point.

2. Realizations of metal fixed points for resistance thermometry

The following subsections describe ways of obtaining metal fixed points having extended regions of reproducible and virtually uniform temperature. Note that there will be very slight vertical temperature gradients resulting from the effect of hydrostatic pressure on the equilibrium temperatures of the liquid-solid interface being measured [McLaren and Murdock (1960)], see Table 1, and the thermometer must be adequately immersed, see Section 5.3 *Hydrostatic head* and Section 5.4 *Cell-furnace interaction*.

The most accurate realization of a solid-liquid phase transition in a metal is generally in the liquid-to-solid direction, i.e. a freezing point. The highest accuracy measurements are greatly facilitated by establishing two solid-liquid interfaces. The outer one is formed during recalescence following the undercool and moves inwards as the freeze progresses. The second, inner, one immediately surrounding the thermometer well is essentially static, and is formed by the insertion of one or more cold brass or fused-silica rods, depending on the temperature of use, immediately following recalescence.

Table 1. Effect of pressure on the temperatures of some defining fixed points. Note that the reference pressure for melting and freezing points is the standard atmosphere ($p_0 = 101\,325\text{Pa}$). For triple points (tp) the pressure effect is a consequence only of the hydrostatic head of liquid in the cell. The values for (dT/dp) are equivalent to millikelvin per standard atmosphere, and those for (dT/dl) are equivalent to millikelvin per metre.

Substance	Assigned value of temperature $t_{90}/^\circ\text{C}$	Temperature variation	
		with pressure, p $(dT/dp)/(10^{-8}\text{KPa}^{-1})$	with depth, l $(dT/dp)/(10^{-3}\text{Km}^{-1})$
Mercury (tp)	−38.8344	5.4	7.1
Gallium	29.7646	−2.0	−1.2
Indium	156.5985	4.9	3.3
Tin	231.928	3.3	2.2
Zinc	419.527	4.3	2.7
Aluminium	660.323	7.0	1.6
Silver	961.78	6.0	5.4

It should also be remembered that neither melting nor freezing temperatures are completely constant over the whole transition. Evidence of the quality of a melt or freeze comes from careful examination of the shape of the melting or freezing plateau. Repeatable results (often approaching 0.1mK) may be obtained:

- during the 50% of the freeze following recalescence, or
- by specifying that the required temperature is that at which a particular fraction, say 50%, of solid is melted or frozen, see also Section 5.4 *Determination of solid fraction*, and the discussion in Subsection 2.4 *Melting curves* of Guide [Section 2.1 Influence of impurities](#).

In general the freeze is preferred because it is more repeatable. However, in the case of gallium of high purity, the melt is very repeatable and is preferred for practical reasons because the large undercool makes it difficult to initiate a freeze.

3. Fixed-point cell assembly

For calibration of a standard platinum resistance thermometer to the highest accuracy, all metal ingots should be nominally better than 99.9999% pure. Freezing point temperatures below 420°C should then be within a few tenths of a millikelvin of that of an ideally pure ingot. Zone-refined Sn and Zn with a purity of 99.999% will usually allow calibration to within 1mK, but this depends upon the particular impurities present, but see Connolly and McAllan (1980) for a discussion of this question. With Al and Ag (also Au and Cu) a purity of 99.999% will usually result in an error of a few millikelvins. The effect of impurities on the liquidus temperature is discussed in detail in *Guide* Section 2.1 *Influence of impurities*.

For most metal fixed points, the ingot is contained in a cylindrical graphite crucible of high purity (greater than 99.999%) and high density (greater than 1.9gcm^{-3}). For mercury, however, a cell of stainless steel (Type AISI 304) or borosilicate glass is used, while for gallium a flexible container of polytetrafluoroethylene (PTFE) or Teflon is generally preferred, to accommodate the expansion which occurs on freezing. Some success has been reported with stainless steel cells for In, Sn, and Al fixed points [Li *et al.* 2004].

The metal fills the cell or crucible to within about 10mm of the lid, and the thermometer is inserted in a well which reaches down to about 10mm from the bottom, see Figure 1 to Figure 4. The well forms the inner boundary of the cell, within which the atmosphere is controlled. The depth of the thermometer immersion should not be less than 18cm if the highest accuracy measurements are to be achieved. For a discussion of thermometer immersion see Section 5.3 *Hydrostatic head*.

Typically, a graphite crucible is about 45mm in diameter with a wall thickness of about 7mm. The crucible is capped with a graphite lid having a central hole which allows a graphite re-entrant tube of inner diameter of about 10 to 12mm to be axially located in the ingot, see Figure 2. With a thickness of ~8mm for the ingot, the volume of metal would then be of the order of 100cm^3 . The crucible is contained in a closed Pyrex or fused silica tube (commercial metal-clad cells are also available), and the thermometer well inside the crucible assembly is also a closed Pyrex or fused silica tube. The Pyrex and fused-silica glassware are cleaned with diluted nitric acid for a minimum of two hours, and then rinsed intensively with distilled water. In an ‘open’ cell the tubes are sealed by a top-cap cell which allows the interior to be evacuated and back-filled with the appropriate pressure of an inert gas such as argon on each occasion of use. In a sealed cell the tubes and the cap are permanently fused together at the time of manufacture, at the fixed point temperature, after the atmosphere has been set. All graphite components should first have been baked at a temperature at least 20°C above the fixed point temperature under vacuum for more than 24 hours.

3.1. Construction, filling, and realization of sealed triple-point cells suitable for Hg

Sealed cells are not recommended for the realization of the ITS-90 fixed point cells because the pressure within the glass envelope cannot be checked, but they may be used for dissemination of the temperature scale, see [Appendix 1](#). Typical examples of the construction of mercury cells are given by [del Campo *et al.* (2008), Furukawa (1982), Hill (1994), Pavese *et al.* (1999), Strouse and Lippiatt (2001), Steele and Hill (2002), Chattle and Butler (1988), Kalemci *et al.* (2009)]. Borosilicate glass is typically used for the distillation apparatus, and the cell is either borosilicate glass or Type AISI 304 stainless steel. The glass cell, typically having an

outer diameter 30mm and wall thickness 2mm, is filled with about 1.5kg of mercury, which provides an immersion depth of about 18cm [del Campo *et al.* (2008)]. Gently vibrating and rotating the cell during the evacuation process after filling helps to remove air bubbles formed inside the cell. A cold trap containing a refrigerated carbon filter (e.g. sintered charcoal) must be placed between the distillation rig and the vacuum pump to prevent emission of mercury vapour. The filling port above the cell is sealed once the cell is full and evacuated. An example of cell design and distillation apparatus is shown in Figure 1.

Mercury with about 1 part in 10^8 total impurity content can be prepared by filtration and chemical washings plus triple distillation. Chemical washing steps consist of agitation in potassium or sodium hydroxide solution and agitation in dilute nitric acid, with bubbling air through the mercury and thorough rinsing with distilled water. At such high levels of purity both freezing and melting techniques yield triple-point values within about 0.1mK over most of the liquid-solid range [Chattle and Butler (1988), Furukawa (1982), Kalemci *et al.* (2011)].

Mercury cells are nearly always sealed as this is reliable and convenient, and it avoids moisture condensation and contamination of the mercury. Stainless steel cells are to be preferred, as mercury in borosilicate glass cells has been found to undercool up to about 6°C, while that in stainless steel cells undercools only 0.1°C to 0.3°C. Some insulation is needed between the cell and the bath, so that if the surrounding temperature is not controlled precisely, or differs markedly from the triple point, the temperature variations do not significantly influence the measured temperature. On the other hand, too much insulation would make precooling time-consuming. Suitable conditions are conveniently achieved if the cell is contained in a stainless steel or glass tube with a few layers of tissue paper or a thin layer of PTFE insulation between them. Borosilicate cells must be contained in a protective steel enclosure in case of fracture.

The insulation of either type of cell may also be controlled if there is provision for varying the pressure in the annular space between the holder and the cell. Ethyl alcohol is used in the thermometer well to improve the thermal contact with the thermometer. A controlled environment, such as a stirred ethanol bath, is normally used for the realization.

Alternatively, a mixture of solid CO₂ and ethyl alcohol can be used for cooling, the stainless steel holder being immersed in the cooling mixture. In the procedure described by Furukawa [Furukawa 1982], the annular space is evacuated when the cell temperature reaches the freezing point. When the mercury has begun to freeze or is in the undercooled state, the thermometer is removed and (in some laboratories) an auxiliary closed-end thin-wall stainless steel tube is inserted into the thermometer well. Two liquid nitrogen cooled glass rods successively inserted into the stainless-steel tube will produce a solid mercury mantle on the thermometer well. The stainless-steel tube is then withdrawn, taking with it any ice that may have been introduced by the glass cooling rods. Finally, the thermometer, which has been pre-cooled in an auxiliary alcohol-filled tube immersed in the solid CO₂ ethyl-alcohol cooling mixture, is inserted into the thermometer well. With continuous evacuation of the annular space, freezing times of up to 14 hours have been obtained using about 2kg of mercury in the cell. The repeatability of the triple point on freezing is better than about 0.05mK.

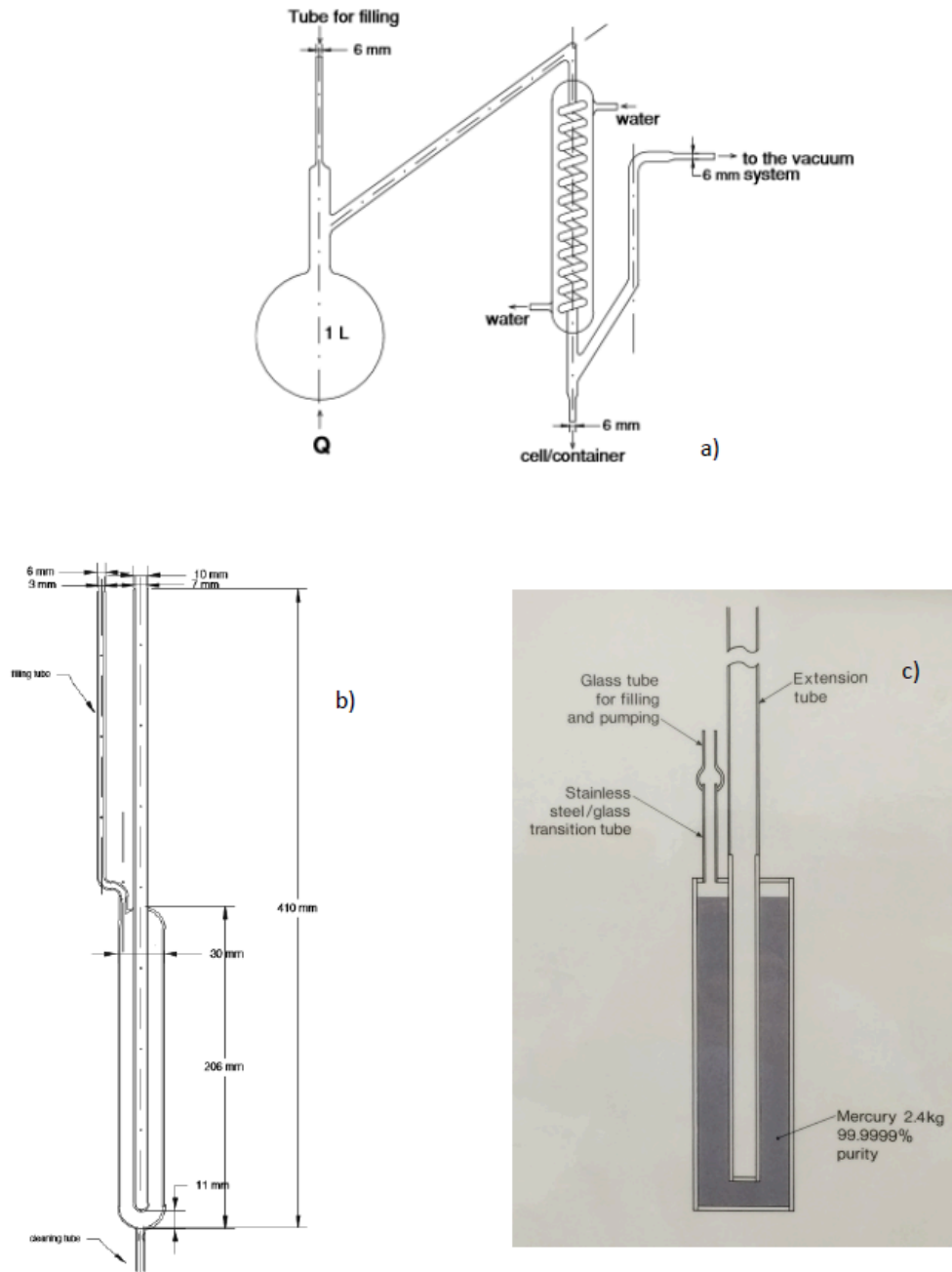


Figure 1 — Distillation apparatus for mercury cells (a), and design (b) [del Campo_et al.(2008)]. c) *Stainless-steel mercury cell.* _Illustration reproduced with the permission of Springer: *International Journal of Thermophysics*, "Assembly and Study of Different Mercury Cells with Known Impurity Content and Isotopic Composition", vol. 29, 2008, pp. 93-103, authors: D. del Campo, V. Chimenti, J. Reyes, J.A. Rodriguez Castillon, M. Moldovan and J.I. Garcia Alonso.

To obtain a triple point realization, the mercury is first frozen rapidly by admitting air to the annular space or with a heat-pipe cooler in the thermometer well. With either method, about 20 to 25 minutes are required from the start of freezing to its completion. The triple point measurements should be carried out either with the annular space around the ingot evacuated, or with the ingot container placed in a plastic foam box to provide adequate thermal

insulation. To start the triple point measurements, warming rods are introduced or a small heater is used until an inner phase boundary around the thermometer well is obtained. The fixed point's check-thermometer or a monitoring thermometer which has been used in earlier measurements will help in testing for the existence of the triple point. Triple point realizations lasting up to 100 hours have been obtained depending upon the thermal insulation. It has been suggested that the largest contribution to uncertainties for the Hg fixed point arises from chemical impurities and the hydrostatic correction (which is large because of the high density of mercury) [Hermier and Bonnier 1992]. Nevertheless, an uncertainty of 0.2mK is achievable for the calibration of Standard Platinum Resistance Thermometers (SPRTs) which is comparable to that achievable with other ITS-90 fixed points.

3.2. Construction, filling, and realization of fixed-point cells suitable for Ga

Typical examples of the construction of gallium cells are given by [Bojkowski *et al.* (2008), Nakano *et al.* (2008), Ranostaj *et al.* (2011), Strouse (1999)]. In general the container, typically made of Teflon or PTFE, is loaded with shot or some other form of the pure metal, inside an argon-filled glove box. It is then removed from the glove box and melted inside a heater unit while under vacuum or inert gas atmosphere. As the metal pieces generally take up more volume than that of the final ingot, the procedure is repeated until the crucible contains the required volume of metal. The crucible is closed at the top with a suitable PTFE or Teflon cap which includes the thermometer re-entrant well. It is then carefully fed into a fused silica or stainless steel holder (Figure 2, see p. 12), or it may be inserted directly into an oil bath or heating unit for the realization of the melting point. The cap may seal the cell [Bojkowski *et al.* (2008)], or allow connection to a gas handling system for control of the atmosphere and monitoring of pressure [Nakano *et al.* (2008), Ranostaj *et al.* (2011)]. A new approach has been outlined using a dry-box system which enables the entire preparation apparatus and heating unit to be kept within a controlled atmosphere [Bojkowski *et al.* (2008)]. Before use, silicone oil is transferred into the re-entrant well to improve the thermal contact between the SPRT and the inner liquid-solid interface.

Gallium with about 1 part in 10^7 total impurity content is commercially available. A sample of this purity allows one to achieve an exceptionally stable melting point [Arai and Sakurai (1990), Bonhoure and Pello (1983), Chattle *et al.* (1982), Mangum and Thornton (1979), Mangum (1982), Nakano *et al.* (2008)]. Gallium melting point cells are commercially available.

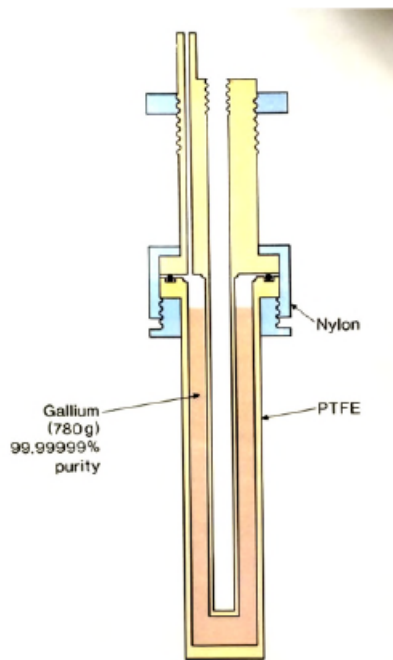


Figure 2 — Gallium melting and triple-point cell.

The large expansion at solidification (3.1%) makes it desirable to use a slightly flexible construction, so an all-plastic container is commonly used, with the parts joined together by means of a high-vacuum epoxy adhesive or a rubber O-ring seal. The plastic is permeable to air, so it is convenient to store and use the cell with the gallium in an atmosphere of pure argon. Gallium shows substantial undercooling (approaching $\sim 30^{\circ}\text{C}$), so the melting transition is used rather than the freezing point. Cells typically contain about 1 kg of gallium.

The gallium is solidified completely by placing the cell in a vacuum flask filled with crushed ice for at least three hours, or by other means as appropriate. Most automatic systems have a mechanism for freezing the gallium.

The re-entrant well is either filled with silicone oil or ethyl alcohol during the realization. The cell containing solid gallium should be placed in the oil bath or heating unit at about 40°C for about 45 minutes to establish the formation of an outer liquid-solid interface. The setpoint is then reduced to 29.9°C , and a small electric heater is placed in the thermometer well [Strouse (1992), Bojkovski *et al.* (2008)]; approximately 10 W is applied for about 20 minutes in order to create a liquid-solid interface adjacent to the thermometer well. An alternative method is described by Marcarino *et al.* (2003), where a differential thermocouple between the sample holder and a shield around it, within the overall enclosure, is used for thermal control.

A pre-heated thermometer is inserted and measurements are started about 20 minutes later. Measurements can be made with several thermometers successively on the same melting plateau which can last up to 50 hours. Standard deviations in the range from $25\mu\text{K}$ to $85\mu\text{K}$ can be achieved for repeated measurements with an individual thermometer [Mangum and Thornton (1979)]. A check for the stability of the gallium cell has been proposed in [Steur and Dematteis (2011a)]. A realization of the triple point of gallium has been presented in [Strouse (1999)].

3.3. Construction, filling, and realization of fixed-point cells suitable for In, Sn, Zn, Al, and Ag

3.3.1. Construction and filling of open cells suitable for In, Sn, Zn, Al, and Ag

Open metal fixed point cells include a connection with a valve for pumping and refilling the cell with argon (or other inert gas) on each occasion of use. This has the great advantage that the pressure in the cell can be set and measured each time, and that possible gaseous impurities that have accumulated can be eliminated. The graphite crucible is usually contained in a Pyrex or fused silica holder long enough to extend to the top of the furnace; this facilitates control of the atmosphere in the cell and provides a means for removing the crucible from the furnace.

The holder is sealed at the top with a stainless steel or brass head, or silicone stopper that provides for the introduction of a suitable inert gas: helium or nitrogen may be used for tin and zinc; argon is used at higher temperatures and may of course be used at any. The oxygen and water content of the gas should in general not exceed ten parts per million, and for metals where reactions are known to occur with these gases (e.g. Al, Ag, Cu) it should preferably be at the one part per million level or better. Hence, a filter can be used to trap trace levels of oxygen present in the argon gas, along with a cold trap.

Cell construction is comparable for all metal fixed points; detailed accounts may be found in [da Silva and Teixeira (2013), Steur and Dematteis (2011b)] and [Widiatmo *et al.* (2006)]. The following instructions correspond to the schematic shown in Figure 3. Bake the high purity graphite parts (crucible, lid, and well) at a temperature of 20K or more above the fixed point under preparation; evacuate the system down to a pressure of 10^{-4} Pa, cool, and fill with pure Ar at about 10^5 Pa (Step 1). Insert the high purity metal into the crucible, put the lid on the crucible, insert the graphite well through the hole in the lid, letting it rest on the metal block, or shot (Step 2). A quartz press-rod is fed through a vacuum-tight seal and rests on the top of the graphite well. Evacuate the auxiliary quartz vessel to a pressure of 10^{-4} Pa, then fill with pure Ar at a pressure of about 90kPa. Then, melt the metal completely; heat it to a temperature of 10K or more above the melting point; push the quartz sheath press-rod downward, until the graphite well reaches the bottom of the crucible (Step 3) and pull it up about 10mm to allow the metal to surround also the bottom of the thermometer well. Allow to cool. If metal shot is used, it will be necessary to add more metal and repeat the procedure until the ingot is complete. If there are concerns about oxygen ingress during melting, the operation may be done under the same conditions as fixed-point realization, i.e. slightly above ambient pressure.

Variations using a funnel to allow sampling of the prepared ingot for chemical analysis have been presented for e.g. the Ag cell [Widiatmo *et al.* (2008), Widiatmo *et al.* (2011a)] as well as with a pre-machined ingot of Zn [Widiatmo *et al.* (2011b), Widiatmo *et al.* (2006)].

Silica wool insulation (interspersed between graphite disks, sometimes also with thin platinum sheets, for temperatures above 400°C) fills this holder from the top of the crucible to the level of the top of the furnace; however, in the case of aluminium, graphite wool instead of silica wool may be preferred as fine silica wool may fuse and lose its insulating properties [McAllan and Ammar (1972)]. The graphite disks act as heat shunts to thermally temper the sheath of the SPRT and reduce the minimum SPRT immersion required for good thermal equilibrium with the fixed-point metal. For Al and Ag, graphite wool rather than silica wool may be preferred above the graphite crucible. Residual water and oxygen, both highly reactive with molten aluminium, must be removed before melting. In addition, the molten aluminium must not be

allowed to come in contact with the fused silica container; it will adhere tenaciously to the silica, and the rapidly following chemical reaction may perforate the container. There have been reports about possible diffusion of sodium from the surrounding heat pipe to the fixed-point metal [Renaot (2008)]. It has also been suggested that the use of nitrogen instead of argon may affect the fixed-point temperature [Petchpong and Head (2007)], but the effect seems to be moderate, only 1.5mK [Renaot and Martin (2009)].

Except in the regions alongside and a little above the sensor, the outer surfaces of both the containing tube and the thermometer well should be roughened so as to prevent heat loss by “radiation piping”. See also Section 5.6 *Light piping* for the effects of radiation heat loss down the sheaths of SPRTs. A typical open cell assembly is shown in Figure 3.

3.3.2. Construction and filling of sealed cells suitable for In, Sn, Zn, Al, and Ag

Sealed metal freezing point cells [Furukawa (1974), Sostman (1977), Ancsin (1985, 1989, see p. 31), Crovini *et al.* (1987), Nubbemeyer (1990)] are also widely used. In these cells, see Figure 4, the fused silica (or Vycor) holder (with cap) and the re-entrant well of the same material are sealed together, forming one integral part hermetically enclosing the graphite crucible, the graphite re-entrant well, and the metal ingot under pure argon at the appropriate pressure. The following notes give a detailed description of the preparation of a sealed cell. The numbers correspond to those shown in Figure 4.

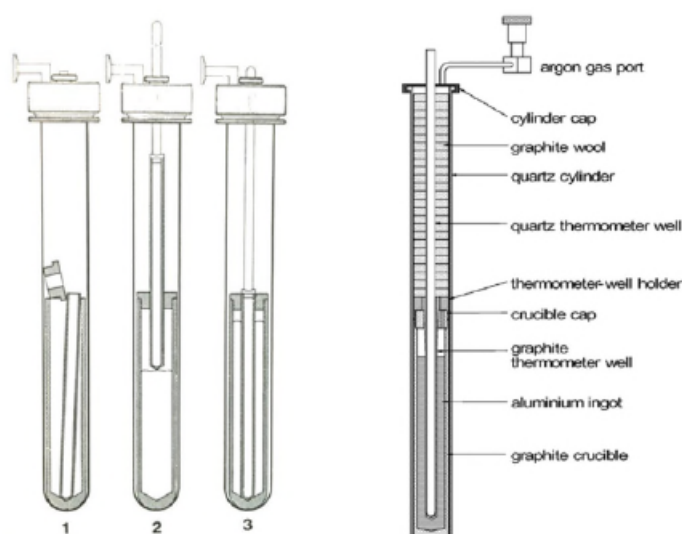


Figure 3 — Open cell construction steps 1 to 3 (left [Nubbemeyer (1990)]) and finished assembly (right [Widiatmo *et al.* (2006)]). (*Illustration to the right is reproduced by permission of IOP Publishing. All rights reserved. [Widiatmo *et al.* (2006)].*)

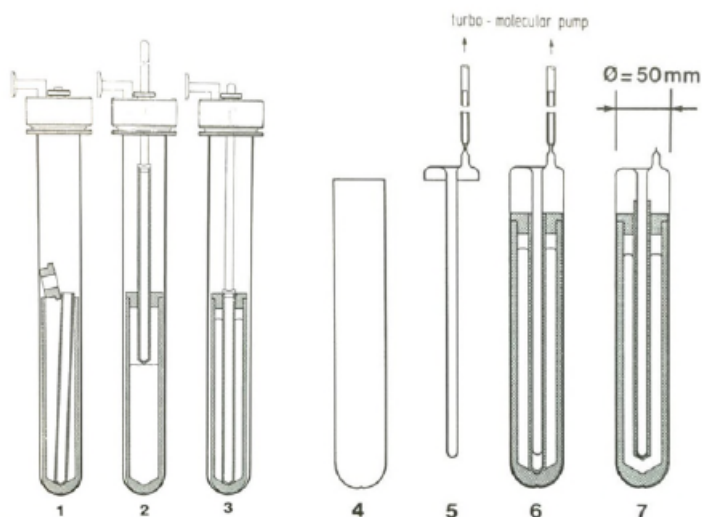


Figure 4 — Preparation and filling of a sealed cell suitable for the freezing points of In, Sn, Zn, Al, and Ag [Nubbemeyer (1990)]: (1) Parts ready for baking in vacuum. (2) Join the graphite parts and the metal block (or shot) of the fixed-point cell. (3) Melt the metal block and lower the graphite well completely. (4) and (5) Quartz parts ready for degreasing. (6) Assemble crucible and quartz parts, seal the quartz, evacuate and fill with argon. (7) Seal off.

Preliminary phase

- 1 Bake the high purity graphite parts (crucible, lid, and well) at a temperature of 20K or more above the fixed point under preparation; evacuate the system down to a pressure of 10^{-4} Pa, cool, then fill with pure argon at about 10^5 Pa.
- 2 Insert the high purity metal into the crucible, put the lid on the crucible, insert the graphite well through the hole in the lid, letting it rest on the metal block. A quartz press-rod is fed through a vacuum-tight seal and rests on the top of the graphite well. Evacuate the auxiliary quartz vessel to a pressure of 10^{-4} Pa, then fill with pure argon at a pressure of about 90kPa⁽¹⁾.
- 3 Melt the metal block completely; heat it to a temperature of 10K or more above the melting point; push the quartz sheath press-rod downward, until the graphite well reaches the bottom of the crucible.

Second phase

- 4 and 5 Degrease the lower and upper part of the quartz sheath shown using ethanol, etch it (

⁽¹⁾ Due to the high vapour pressure of zinc at its melting point and the tendency of molten aluminium to bond to graphite in vacuum, both of these metals should be melted only in the presence of about one atmosphere of a gas such as argon.

6 and 7

5% fluoric acid, 5 minutes), and rinse about ten times with high purity water.

Assemble the two parts of the quartz sheath and the crucible prepared as above; fuse the quartz parts together. Assemble the cell in a holder and lower into the furnace. Evacuate it to a pressure of about 10^{-4} Pa by means of a turbo-molecular pump. Insert a calibrated platinum resistance thermometer into the quartz well of the cell. Melt the fixed-point metal completely, until the graphite well floats up from the base of the crucible by about 10 mm allowing the metal to surround the bottom of the thermometer well. Let the fixed-point metal freeze slowly, filling the cell with argon at a pressure of 95 to 100 kPa. While keeping the cell close to the freezing point temperature, seal off the pump tube directly above the furnace (the actual values of the filling pressures and seal-off temperatures, here and elsewhere, should be such that the pressure at the freezing-point temperature is well within 1% of one standard atmosphere, see Table 1, see p. 6)

Great care must be taken with sealed cells because the gas pressure within cannot be measured after sealing. In particular, some suppliers are located at high altitude and the pressure can be as much as 20% lower than atmospheric pressure at sea level. In that case the supplier's certificate should state the pressure in the cell and the corresponding freezing temperature. In service, a sealed cell should periodically be compared against a reference cell to verify that the freezing temperature has not changed, for example due to build-up or loss of pressure in the cell. See the detailed discussion in [Appendix 1](#).

3.3.3. Realization of the freezing point of indium (156.5985°C)

The goal of the realization procedure for all the metal fixed point cells is to establish two liquid-solid interfaces: an inner interface, which completely surrounds the thermometer well, is equidistant from it at all points, and remains almost completely static during the solidification process; and an outer interface, which propagates inwards from the outer edge of the ingot. The outer interface is established by reducing the furnace temperature and allowing nucleation to occur spontaneously at the interface between the ingot and the graphite surface (except where otherwise specified in the following descriptions). The inner interface is generally established by insertion of one or more cold rods, such as a cold thermometer or brass rods cooled by immersion in liquid nitrogen. This rapidly sets up a thin region of solid adjacent to the thermometer well.

Freezing-point cells of a conventional graphite crucible containing high purity indium (greater than 99.999%) have been described by McLaren (1958) and Chattle and Pokhodun (1989).

Sawada (1982) described a triple-point cell made entirely of glass, while Oleinik *et al.* (1984) and Mangum (1989) reported results obtained from PTFE-encased cells.

A typical procedure is as follows. After melting the ingot and holding it overnight at about 5°C above the melting temperature, the furnace is stabilised a degree or so below the expected freezing point. When the temperature indicated by a check-thermometer in the cell has fallen close to the freezing point the thermometer is withdrawn and allowed to cool for up to 1 minute before being replaced in the cell. The loss of heat to the thermometer is sufficient to cause rapid nucleation with the formation of a thin mantle of solid indium around the thermometer well; the plateau temperature is reached quickly, and the furnace temperature may then be raised closer to the freezing point. About one hour should be allowed for thermal equilibration of the system prior to taking measurements. Alternatively, with the furnace about 0.2°C below the freezing point, one or two cold fused-silica rods may be inserted for two minutes each to begin the nucleation. Several thermometers may be calibrated sequentially in the same freeze, each being pre-heated to minimise cooling of the mantle around the thermometer well.

Thermal contact of the SPRT with the inner liquid-solid interface of the In cell may be improved by filling the re-entrant well with helium at atmospheric pressure of 101.3kPa. For small-diameter SPRTs an aluminium bushing can improve thermal contact, although the design must be carefully considered or they can make the situation worse [Batagelj *et al.* (2011), Steur and Dematteis (2008)].

The freezing point of a high purity (99.9999%) sample of indium is reproducible to about 0.1mK [Mangum (1989)]. The freezing temperature has been found to be somewhat sensitive to the realization technique [Ivanova and Pokhodun 1992].

3.3.4. Realization of the freezing point of tin (231.928°C)

A large undercool occurs when high purity tin freezes. Because of this, in order to obtain a suitable constant temperature plateau, particular care is needed with the nucleation. The procedure of [McLaren (1957), McLaren and Murdock (1960)] is as follows. The ingot is melted overnight. For nucleation of the outer liquid-solid interface, the melted ingot is allowed to cool slowly (less than 0.1K per minute) until its temperature approaches the freezing temperature of the tin. At this point the Pyrex tube holding the crucible of tin and the thermometer is extracted from the furnace block into the opening of the furnace until the top of the crucible is nearly level with the top of the furnace (or, for quicker results but a shorter operating period, extracted completely from the furnace) and is held in this cooler environment until recalescence occurs. The crucible is then immediately lowered into the block, which will still be close to (or may be automatically controlled about 1K below) the freezing temperature. The result of this operation is the formation of a solid shell of tin of approximately uniform thickness at the outer walls of the crucible.

In modern practice, the external nucleation is sometimes done by flowing cold argon around the cell, or it is omitted altogether; the furnace temperature is dropped to about 4°C below the freezing point prior to inner nucleation. For this, the thermometer is withdrawn from the well and one or two cold fused-silica rods are inserted for two minutes each, or a gentle flow of cold air, or nitrogen [Marcarino *et al.* (1992), Marcarino *et al.* (2003)] is introduced into the well for one or two minutes, until nucleation is observed e.g. with a thermocouple at the outside of the fixed-point cell. The thermometer is replaced and the furnace is heated to just below the freezing point whereupon, if nucleation has been successfully achieved, a satisfactory plateau follows. Otherwise the procedure may be repeated.

It is important to achieve a high degree of undercooling ($> 4\text{K}$) for the attainment of the plateau temperatures by means of outside-nucleated slow freezes. High-purity tin should be kept in an inert atmosphere. To reduce the magnitude of the undercool required, Zhang and Wang (2008) have reported success with graphite powder addition, which eliminates the need for the ‘outside nucleation’ technique. Tin (and to a smaller degree also zinc) has been observed to seep with time (tens of years) through the graphite wall for heavily used fixed-point cells [Steur and Dematteis (2011b)], possibly also giving rise to inadequate undercooling.

The extent of the undercool appears to depend on the characteristics of the previous overheating. Ingots that are held 10K above their liquidus points overnight nearly always supercool more than those that are refrozen less than 2 hours after melting. When ingots are held 2K or less above the liquidus points for 2 hours or less and then refrozen, the observed undercooling is usually less than 4K . It has also been reported [Marcarino *et al.* (1992), Marcarino *et al.* (2003)] that a satisfactory inner-nucleated freeze can be obtained following nucleation induced by a flow of cold nitrogen into the thermometer well.

The freezing point of high purity (99.9999%) Sn is reproducible to within about 0.1mK .

Depending on the thermometer construction, it may require as little as 13cm or as much as 25cm immersion in the constant temperature zone; in general, at least 18cm is recommended.

3.3.5. Realization of the freezing point of zinc (419.527°C)

The freezing temperature is obtained as follows [McLaren (1957), McLaren (1958)]. The ingot is melted overnight. The melted ingot is allowed to cool until nucleation at the outside of the ingot begins, as evidenced by an initial arrest in the cooling curve. The thermometer is then withdrawn from the well for about 1 minute (during which time the temperature indication drops below 200°C) and replaced. If the thermometer is held in the room for much more than 1 minute an unnecessarily large amount of the sample is frozen on re-insertion, and the recovery time is extended. The loss of heat to the thermometer causes rapid nucleation and growth of a mantle of solid zinc about 1mm thick on the thermometer well, the solid-liquid boundary of which constitutes the zinc point interface around the sensing element of the thermometer. Thereafter this interface remains nearly stationary; the bulk of the metal freezes (un-nucleated) in a cylindrical shell from the crucible walls.

When many thermometers are calibrated using the same freeze, the thermometers should be pre-heated close to the zinc point to avoid changing the thickness of the solid zinc mantle on the thermometer well. The apparent reproducibility of the freezing point from sample to sample of 99.9999% Zn is of the order of 0.2mK .

Depending on the thermometer construction, it may require as little as 18cm immersion in the constant temperature zone; some types require 25cm immersion.

3.3.6. Realization of the freezing point of aluminium (660.323°C)

The ingot should first be completely melted by keeping it at a temperature about 10°C above the freezing point for about 2 hours.

The ingot is allowed to cool slowly (about 0.1K per minute) below the freezing point. It usually undercools about 0.4 to 0.6K . When recalescence is observed, the thermometer is removed and the cooled thermometer or a fused silica rod is re-inserted in order to generate an inner solid aluminium mantle on the well. The temperature of the furnace should then be set 0.5

to 1K below the freezing temperature. Depending upon the purity of the aluminium sample, the temperature is constant to about 0.2mK over the first 50 percent of the freeze [McAllan and Ammar (1972), Furukawa (1974)]. The reproducibility of this point in any one laboratory may be about 1mK, the measurements being limited by the stability of the thermometers used.

3.3.7. Realization of the freezing point of silver (961.78°C)

The ingot should first be completely melted by keeping it at a temperature about 10°C above the freezing point for about 12 hours.

The recommended induced-freezing technique is similar to that used for the freezing point of zinc or aluminium. The ingot is allowed to cool slowly (about 0.1K per minute) below the freezing point; at such a low cooling rate the undercooling never exceeds 0.5K. When it is evident nucleation is taking place (the temperature rise clearly shows the recalescence) the thermometer is extracted from the well and then reinserted after about 1 minute exposure to ambient temperature.

After the temperature has risen to a steady value on the plateau, it remains constant to within 1mK or better for a further 40% or more of the total freezing time.

The presence of oxygen in the silver will lower the observed freezing temperature. Experiments with argon-oxygen mixtures (up to 1% oxygen) bubbling through the silver have produced liquidus point depressions that were always less than 5mK. A slope inversion on a melting curve following a very fast freeze is a reliable indication of contamination by oxygen. However, if the ingot is kept in the molten state in an inert gas the surrounding graphite will effect the complete removal of the oxygen within a few hours [Bongiovanni *et al.* (1975), Takiya (1978)].

4. Apparatus

4.1. Liquid comparison baths (triple point of mercury)

A common option for realization of the mercury triple point or melting point is immersion of the fixed-point cell in its holder in a stirred temperature-controlled bath (of order 40 litres) of liquid such as acetone or ethanol. Various baths are commercially available which provide an isothermal environment by automatically stirring the liquid and maintaining a specified temperature by a two-stage compressor system and heater. A bath depth of about 50cm is desirable. With this system a mercury triple point (melting or freezing) plateau can be realized with a duration of several days or even a week. A typical stirred liquid bath is shown in Figure 5. A dry-cooler technique has also been demonstrated [Gam *et al.* (2004)].

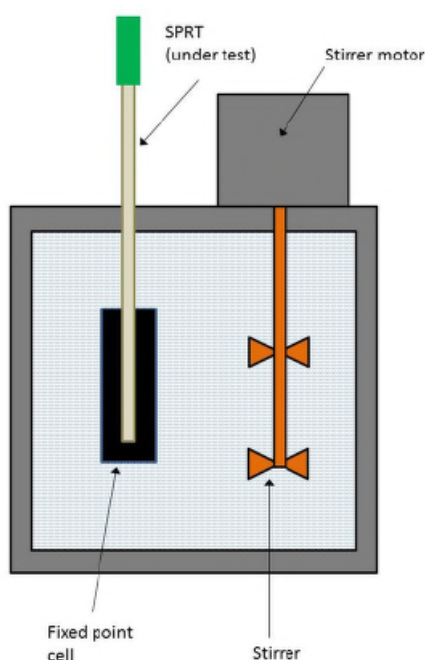


Figure 5 — Typical stirred liquid bath.

4.2. Automatic realization apparatus (melting point of gallium)

In addition to the liquid comparison bath (using silicone oil), various types of apparatus dedicated to the realization of the gallium fixed point are commercially available. These typically contain a large cylindrical metal block with a central well for the Ga cell. A single-zone, wound DC heater wire on the metal block controls the temperature. The annular space between the cell and the metal block should be minimised; a gap of 1mm is typical. Coaxial melting over a period between 12 hours and 24 hours is generally performed automatically. On re-freezing, a slight temperature variation along the cell axis is required to ensure that freezing occurs preferentially from bottom to top to prevent damage to the cell due to the expansion of gallium. When the gallium point is realized using the differential thermocouple method [Marcarino *et al.* (2003)], a dedicated apparatus for its realization is not needed.

4.3. Medium temperature furnace (freezing points of In, Sn, Zn)

A furnace suitable for metals which freeze below about 500°C is shown in Figure 6. The tube containing the crucible fits into an aluminium block which is centred in a ceramic tube heated by a nickel-chromium winding powered by a regulated supply. Commercially available furnaces dedicated to this purpose typically have three DC heating zones to provide a uniform temperature environment over the length of the fixed-point cell. An example of a well-functioning furnace for the tin fixed point is given by [Yamazawa *et al.* (2007)]. A freezing plateau can be maintained for at least 12 hours with this type of furnace. Instead of an (aluminium) block a heat-pipe can be used with a suitable working fluid, inserted in a single-zone furnace, in order to reduce the vertical gradient in the furnace to the level of 10mK or better.

4.4. High temperature furnace (Al, Ag)

Figure 7 shows a high temperature freezing point furnace. It differs from the medium temperature furnace of Section 4.3 in the following ways: an Inconel lining tube is used or, preferably, a heat pipe; there may be end-heater windings, but generally not when heat pipes are used; fused silica fabrics and sleeveings are used as electrical insulations for the heater windings which can be made from nickel-chromium or Kanthal wires; there are stainless steel or Inconel radiation shields above the cell. Bottom and top supports for the furnace block are Inconel and the outer and inner insulation materials are typically silica wool; exterior water cooling may be desirable in air conditioned laboratories. Further details on high-temperature furnaces are given in [Marcarino *et al.* (2003)].

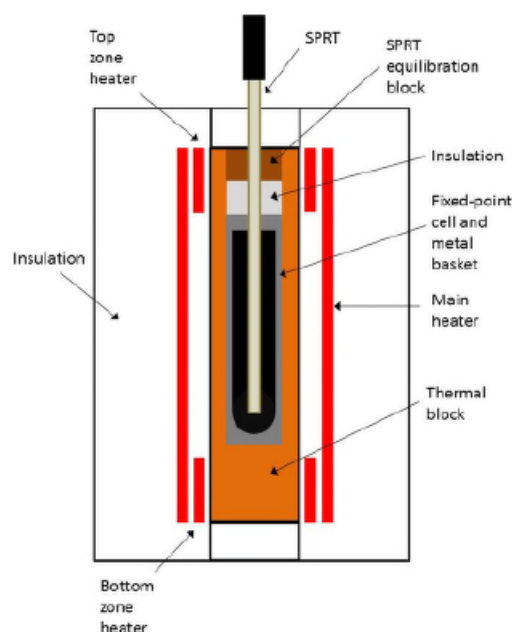


Figure 6 — Medium temperature three-zone furnace for resistance thermometry metal freezing points.

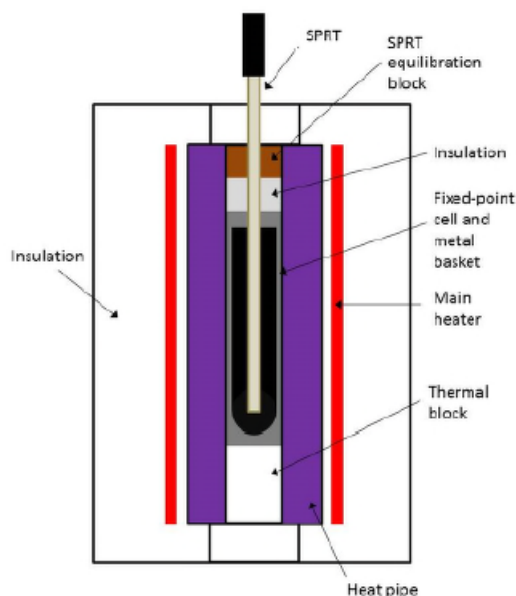


Figure 7 — High temperature furnace for resistance thermometry metal freezing points. A heat pipe is preferred, but is a much more costly alternative to the Inconel block; with a heat pipe, the end heaters are omitted.

When using resistance thermometers with AC bridges at frequencies above 10Hz, it is advantageous to have non-inductive windings for the heaters. Control systems should be designed so that any switching is done at zero current, to reduce electrical interference; interference is adequately suppressed if there is no change in the measurement when the furnace power is switched off for a short period.

Heat pipes are highly effective devices for transferring heat using the vaporisation and condensation of fluids to transport heat with small temperature drops. Using different ‘working fluids’, heat pipes can operate over a range of temperatures. Heat pipes with an annular (double-walled cylindrical) geometry that operate over the temperature range from 100°C to 350°C (diphenyl ether), 350°C to 800°C (potassium), and 600°C to 1100°C (sodium) are widely used as furnace liners for temperature metrology to produce stable and uniform temperature zones [Strouse (1992), Marcarino *et al.* (2003)]. The heat pipe may be placed in a conventional single-zone tube furnace. Heat pipes containing mixtures of working fluids have also been investigated [Chen *et al.* (2001)]. A summary of state-of-the-art techniques for heat pipe construction and performance is given by [Yan *et al.* (2011)]. The temperature ranges for typical heat pipes are shown in Table 2.

Table 2. Useful combinations of working fluid, wall material and temperature ranges[after Neuer and Brost (1975)].

Working fluid	Wall material	Useful temperature range (°C)
Freons	Copper, aluminium	−150 to 30
Ammonia	Stainless steel, nickel aluminium	−40 to 60
Acetone	Copper, stainless steel	−40 to 150
Methanol	Copper, nickel	−30 to 150

Working fluid	Wall material	Useful temperature range (°C)
Water	Copper, nickel, titanium, stainless steel	30 to 180
Organic fluids	Stainless steel, super alloys, carbon steel	130 to 300
Mercury (with additives)	Stainless steel	180 to 500
Caesium	Stainless steel, nickel	400 to 600
Potassium	Stainless steel, nickel	400 to 800
Sodium	Stainless steel, nickel	600 to 1050

5. Analysis of performance and estimation of uncertainties

5.1. Purity

While the freezing plateau is used to provide the most repeatable fixed point temperature, the melting plateau provides a great deal of qualitative information on the content and distribution of impurities in the ingot [Quinn (1990)]. Chemical analysis is useful in the initial selection of high purity material, but should be used with caution, and it is advisable to employ complementary methods to give more information on the purity of the cell (see *Guide* Section 2.1 *Influence of impurities*). The advantage of the melting curve over the freezing curve as a source of information on impurity content and distribution is that there is no equivalent of the supercooling and nucleation effects which distort the first part of the freezing curve. Also, since the diffusion of impurities within the solid during melting is much too slow to allow proper equilibrium (i.e., uniform distribution) to be attained throughout the bulk of the ingot, it follows that the solid ingot retains information concerning segregation of impurities during freezing; some of this information can be obtained from a comparison of melting curves following various rates of freezing. Many examples are given by McLaren (1962). A full discussion of purity effects is given in *Guide* Section 2.1 *Influence of impurities*.

5.2. Temperature stability and uniformity

It is important to understand the thermal characteristics of the furnace and liquid baths with the fixed-point cells installed, to minimise their impact on the fixed-point cell realization temperature and to minimise the risk of damage to the cells during use [Strouse and Furukawa (1999), Strouse (2004)]. The temperature stability of the furnace or bath, as well as the vertical temperature profile, may be determined by setting the temperature of the device about 2°C below the fixed-point temperature. Single-phase materials do not exhibit observable hydrostatic-head effects in the vertical temperature profile.

The temperature stability is determined by placing an SPRT into the re-entrant well of the fixed-point cell and measuring the temperature fluctuations for at least 12 hours. In general, depending on the furnace, the temperature fluctuations should not cause the SPRT readings to vary by more than about $\pm 10\text{mK}$.

The vertical temperature profile over the length of the fixed-point crucible is determined by slowly inserting the SPRT into the fixed-point cell in 2cm steps over the length of the crucible. At each step, the SPRT should be allowed to equilibrate for five minutes prior to taking the measurement. In general, the vertical temperature variation should not exceed about $\pm 10\text{mK}$. An example measurement of the vertical temperature profile is shown in Figure 8.

⁽¹⁾ Illustration reprinted with permission from G. Strouse.

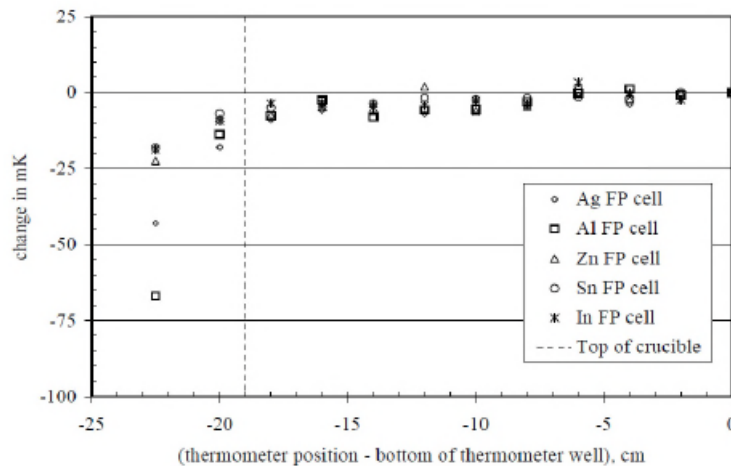


Figure 8 — Vertical temperature profiles for several fixed-point cells, with furnace temperature 2.5°C below the freezing point of the fixed-point cell. The thermometer position is relative to full insertion in the well [Strouse (2008)]⁽¹⁾.

5.3. Hydrostatic head

If the furnace profile is satisfactory, and the SPRT has low stem conduction (axial heat flow) and it makes good radial contact with the thermometer well, then when it is raised in the well during a freeze its reading will track the temperature gradient in the liquid-solid interface caused by the changes in the hydrostatic pressure (see Table 1, see p. 6). This can be demonstrated by performing a measurement of the vertical temperature profile during a fixed-point realization. For the SPRT to be considered properly immersed (i.e. the stem conduction is not influencing the measurement), the thermometer must track the hydrostatic-head effect (see Table 1, see p. 6) over at least the lowest 3cm of the re-entrant well.

This can be verified by measuring the SPRT resistance starting at 10cm from the bottom of the re-entrant well, then inserting it in 2cm steps until 4cm from the bottom, then in 1cm steps until the bottom of the re-entrant well is reached [Strouse (2008)]. When this procedure is performed in the opposite way, by successively extracting the thermometer, more time will be needed for equilibrium due to cold air being sucked in by the thermometer. After each change of immersion depth, five minutes should be allowed for equilibration of the SPRT prior to measurement. Self-heating corrections should be applied. The immersion depth of the SPRT is calculated as the vertical height from the sensor midpoint to the top of the liquid column during the realization. An example measurement of the immersion profile during the realization, for In, is shown in Figure 9. Note that the temperature gradient in the ingot arising from the hydrostatic head effect causes a heat flux which can, in principle, reduce the measured immersion differences [Batagelj *et al.* (2011)].

⁽¹⁾ Illustration reprinted with permission from G. Strouse.

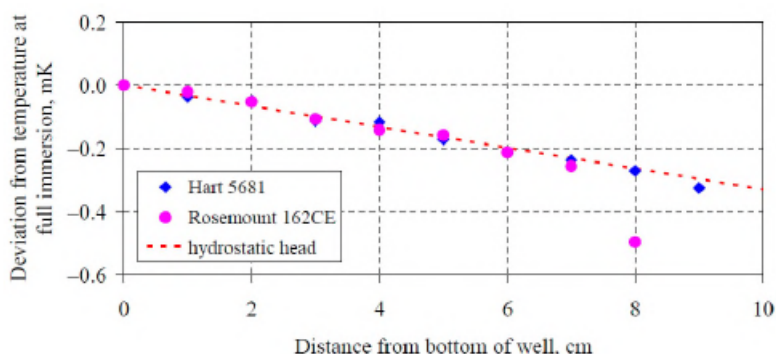


Figure 9 — Immersion profile during realization of In freezing point [Strouse (2008)]⁽¹⁾.

5.4. Cell-furnace interaction

A practical characterisation procedure for fixed points from In to Al was outlined by [Rudtsch and Fahr (2008)]. Two major contributions to the uncertainty when realizing the fixed point are the thermal (i.e. furnace-related) effects and impurity effects. These are often convolved and interacting, so it is important to separate them. To do this, the first thing is to characterise and minimise thermal effects. This requires the adjustment of furnace settings, which depends on the type of furnace and fixed-point cell. In a heat-pipe furnace this is a characterisation of stability and vertical temperature uniformity (see Section 5.2, see p. 24) at a temperature just below the fixed-point temperature. For multi-zone furnaces, the settings of the individual zones must be adjusted to homogenise the temperature profile. One approach is to take the immersion characteristics of the SPRT in the re-entrant well of the fixed-point cell as a measure of temperature homogeneity. However, because of the high thermal conductivity of the fixed-point material, the measured homogeneity appears to be much better than the quantity of interest, which is the temperature homogeneity of the surfaces surrounding the liquid-solid interface. In other words, the information required is the temperature on the outer surface of the fixed-point ingot. It is therefore more appropriate to measure the temperature homogeneity in the gap between the fixed-point cell and the furnace wall, which usually means employing a thermometer with a small outer diameter such as a 100 Ω industrial PRT (space permitting). It is recommended to use both approaches in order to gather information about the temperature profile inside and outside the ingot.

An alternative approach is to measure the temperature at the bottom of the re-entrant well during a complete fixed-point realization for a variety of different heater zone settings: the curve which offers the best approximation to a Scheil curve [Pearce *et al.* (2012)] (i.e. free from spurious effects towards the end of freezing) is likely to indicate the optimum heater zone settings, because the absence of spurious effects (see below) represents the situation where the sensing element of the SPRT is completely surrounded by a liquid-solid interface for the longest time [Pearce *et al.* (2013)].

During the realization of the metal freezes, thermal effects occur, manifesting themselves as spurious (non-Scheil) behaviour in the freezing curves. This is because the SPRT is not completely surrounded by the liquid-solid interface. Depending on their origin, two types of thermal effects can be categorised. The first is the parasitic heat exchange between the sensing element of the SPRT and the surroundings (i.e. the laboratory). This can be due to thermal radiation at temperatures above the Sn point, but also due to losses caused by heat conduction

along the thermometer axis (as discussed earlier). The second type is due to incomplete phase boundaries, both at the beginning and at the end of the fixed-point plateau [Large and Pearce (2014)]. As long as there are gaps in the phase boundary, the temperature measured by the SPRT is an average of the temperature of the phase boundary and the temperature of the outer wall of the fixed-point crucible. In particular, purer fixed-point cells show a considerable influence of thermal effects at the beginning of the plateau. For this reason, particular attention must be paid to the initiation procedure [Abasov *et al.* (2010), Ivanova *et al.* (2013), Large and Pearce (2014), Shulgat *et al.* (2013), White and Mason (2011)]. Identical behaviour might be expected from dendrites acting as thermal bridges across the cell, but it is now considered to be unlikely that dendrites are sufficiently long-lived for this to be significant [Pearce *et al.* (2012), Rudtsch and Fahr (2008)].

A parameter that describes the cell-furnace interaction (i.e. thermal effects) is the so-called ‘penetration ratio’, or ‘attenuation factor’, μ_{furnace} , which is the ratio of the change of measured fixed-point temperature to the change of the furnace temperature [Fahr and Rudtsch (2008)]. If $\mu_{\text{furnace}} < 10^{-5}$, steady-state (static) thermal effects can be ignored. This may be obtained by oscillating the furnace setpoint temperature: if the SPRT sensing element is surrounded by the liquid-solid interface, minimal changes will be observed. In this case, the temperature of the thermometer is determined only by the temperature of the liquid-solid interface, the thermal resistance between the sensing element and the interface, and the thermometer stem losses [Bongiovanni *et al.* (1975), Takiya (1978)]. If the thermometer is not well surrounded by the interface, the furnace oscillations will be prominent in the SPRT measurements (see Figure 10, see p. 27) and remedial action is needed to improve the temperature profile. In intermediate cases, the measured sensitivity to furnace settings can be used to correct the transition temperature for the offset of the furnace temperature with respect to the transition temperature, or to estimate the uncertainty due to this offset.

Note that the thermal conditions (specifically, the morphology of the liquid-solid interface and how it evolves with time) have a profound influence on the behaviour of impurities [Renaot *et al.* (1999), Large and Pearce (2014)], see also *Guide* Section 2.1 *Influence of impurities*.

A further cause of thermal effects is heat conduction along the re-entrant well and the SPRT, which was recently demonstrated to be a more important effect than previously thought, at least for the zinc fixed point [Rudtsch *et al.* (2013)]. It is recommended that SPRTs with inferior immersion characteristics should be calibrated in open zinc cells without a fused silica re-entrant well.

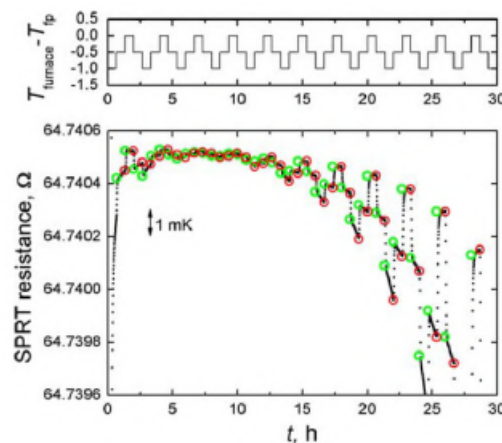


Figure 10 — SPRT resistance as a function of time during Zn freeze, while the furnace temperature is oscillating by $\pm 0.5\text{K}$, indicating a penetration

ratio of ~ 0.01 . *Illustration reproduced with the permission of Springer: International Journal of Thermophysics, "A New Method for the Quantification and Correction of Thermal Effects on the Realization of Fixed Points", vol. 29, 2008, pp. 126-138, authors: M. Fahr and S. Rudtsch.*

5.5. Determination of solid fraction

For the validation of fixed-point cells by thermal analysis, see *Guide* Section 2.1 *Influence of impurities*, it is necessary to convert the time elapsed since the start of freezing to fraction of metal that has solidified (the ‘solid fraction’). As the rate of heat extraction from the ingot is broadly constant, the two quantities are linearly related and the problem is to estimate the solid fraction just after recalescence and to identify the end-point of the freeze. In practice, the start of the freeze can be taken as the point of maximum temperature after recalescence (i.e. in any freeze the sample of interest is somewhat less than the whole). There are three main ways to determine the end-point: experimental detection by measuring furnace power draw; a retrospective determination using spline fits; and an approximate method by determination the point of the inflection as the temperature drops towards the furnace set point after freezing. These three methods can be summarised as follows.

- The experimental method of detecting the end-point of freezing was developed by [Yamazawa *et al.* (2007)] and involves measuring the power drawn by the furnace. During the freezing, the heat extraction rate is constant and so the furnace power is constant. Once freezing is complete, there is a sudden increase in heater power to maintain the furnace at the set temperature (see Figure 11, see p. 28), to compensate for the absence of the heat of fusion. By recording the electrical power drawn by the furnace as a function of time, it is possible to determine the time at which freezing finished. Since the time at the start of freezing is known, it is then possible to deduce the solid fraction as a function of time.

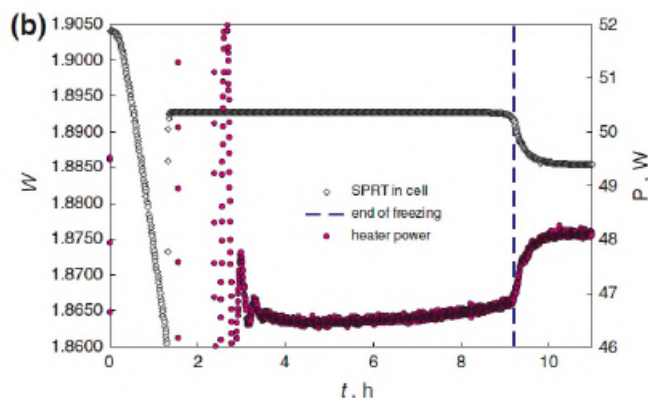
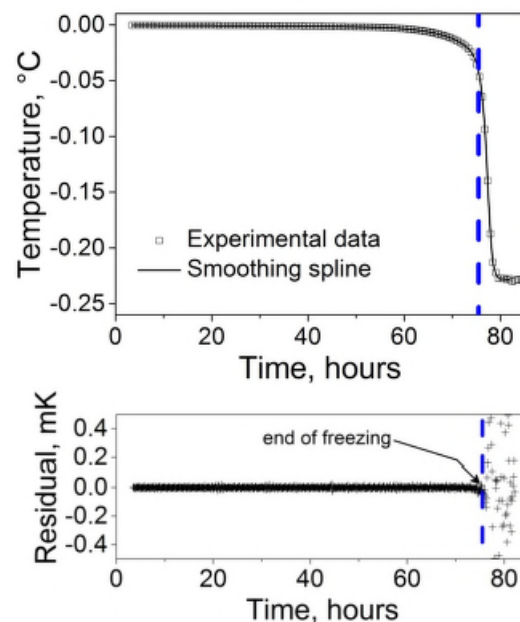


Figure 11 — Determination of endpoint by measuring the heater power (lower trace) concurrently with the SPRT resistance (upper trace, resistance ratio $W = R(t)/R(273.16\text{K})$); the abrupt increase in heater power at about 9 hours indicates the loss of heat flow from the ingot and therefore end of freezing. *Illustration reproduced with the permission of Springer: International Journal of Thermophysics, "Thermal Analysis of the Heater-Induced Realization of the Tin Fixed Point", vol. 28, 2007, pp. 1941-1956, authors: K. Yamazawa, J.V. Widiatmo, and M. Arai.*

- The freezing endpoint can also be determined from the experimental data by deducing the influence of the furnace on the SPRT by characterising the standard deviation of the SPRT measurements [Pearce *et al.* (2013)] in the absence of a heat pipe (which shields most of the variations in the furnace temperature). During the freeze (sensing element in close contact with the liquid-solid interface) this may be of the order of $15\mu\text{K}$, but when the sample is fully solid or fully liquid, most of the observed scatter in the data is due to the fluctuations of the furnace temperature, and the standard deviation is much larger, about $2000\mu\text{K}$. The endpoint can be detected (for example) from the residuals of spline fits [de Boor (1978)] to segments of data as illustrated in Figure 12. Note that the temperature of the freeze at the end-point is some 0.2°C below the initial freezing point.
- It has been observed that in many cases, the freezing endpoint determined with the spline method is located close to the point of inflection in the plateau seen as the SPRT temperature drops towards the furnace temperature (see Figure 12, see p. 29). This suggests that an approximate endpoint can be determined by simply locating this point of inflection.



⁽¹⁾ Illustration reprinted with permission from American Institute of Physics. Copyright 2013, AIP Publishing LLC. This article may be downloaded for personal use only. Any other use requires prior permission of the author and the AIP Publishing LLC.

Figure 12 — Illustration of the spline method for determining the end-point of a freeze. The appearance of 'noise' (i.e. residuals in the spline fits) suggests that the endpoint is at about 76.4h. [Pearce *et al.* (2013)]⁽¹⁾. Note that the end-point of freezing occurs at a temperature way below the plateau (this is also the case for the heater power determination of the end-point in Figure 11, see p. 28).

5.6. Light piping

Radiation heat losses in transparent thermometer sheaths and other transparent components can have a large effect on fixed-point measurements above the Sn point [Evans and Wood (1971), McLaren and Murdock (1966a), McLaren and Murdock (1966b)]. The effect is caused by multiple reflections between the inner and the outer surface (light piping) of thermometer sheaths and fused silica re-entrant wells. It increases with increasing temperature but is

minimised either by blackening or by roughing (sand blasting) the outer surface of SPRTs and the re-entrant well [Rudtsch *et al.* (2013)].

References

- [1] Abasov M Y, Gerasimov S F, Ivanova A G, Pokhodun A I, Shulgat O S 2010 Measurement of Al Freezing-Point Temperature: Effect of Initiation Process, *Int. J. Thermophys.* **31**, 1663-1675
- [2] Ancsin J 1985 Melting Curves and Heat of Fusion of Indium, *Metrologia* **21**, 7-9
- [3] Ancsin J 1989 A Study of the Realization of the Melting and Freezing Points of Silver, *Metrologia* **26**, 167-174
- [4] Arai M, Sakurai H 1990 Development of a sealed glass cell for gallium triple point, TEMPMEKO '90 (Finnish Society of Automatic Control), 80-85
- [5] Batagelj V, Bojkowski J, Drnovsek J 2011 Numerical Modelling of Heat Flux in Fixed-Point Cells Due to the Hydrostatic-Head Effect, *Int. J. Thermophys.* **32**, 2295-2303
- [6] Bojkowski J, Hiti M, Batagelj V, Drnovsek J 2008 New Approach in Filling of Fixed-Point Cells: Case Study of the Melting Point of Gallium, *Int. J. Thermophys.* **29**, 119-125
- [7] Bongiovanni G, Crovini L, Marcarino P 1975 Effects of Dissolved Oxygen and Freezing Techniques on the Silver Point, *Metrologia* **11**, 125-132
- [8] Bonhoure J, Pello R 1983 Température du Point Triple du Gallium, *Metrologia* **19**, 15-20
- [9] de Boor C 1978 *A Practical Guide to Splines* (New York: Springer) p. 211
- [10] Chattle M V 1972 Platinum Resistance Thermometry up to the Gold Point, Temperature, Its Measurement and Control in Science and Industry, *Instrument Society of America* (Pittsburgh) **4**, 907-918
- [11] Chattle M V, Rusby R L, Bonnier G, Moser A, Renaot E, Marcarino P, Bongiovanni G, Frassinetti G 1982 An Intercomparison of Gallium Fixed Point Cells, Temperature, Its Measurement and Control in Science and Industry, *American Institute of Physics* (New York) **5**, 311-316
- [12] Chattle M, Butler J 1988 *Cells for the realization of the triple point of mercury*, NPL Report QU 79
- [13] Chattle M V, Pokhodun A I 1989 An Intercomparison between fixed-point cells made at VNIIM (USSR) and NPL (UK) for the realization of the melting and triple points of gallium and the solidification points of indium and cadmium, *Measurement* **7** (4), 146-152
- [14] Chen Y, Liu Y, Li Y, Jin X, Song H 2001 A medium temperature radiation calibration facility using a new design of blackbody as a standard source, *Meas. Sci. Technol.* **12**, 491-494
- [15] Connolly J J, McAllan J V 1980 Limitations on Metal Fixed Points Caused by Trace Impurities, *Metrologia* **16**, 127-132

- [16] Crovini L, Actis A, Galleano R 1987 A sealed cell for the copper point, *High Temperatures—High Pressures* **18**, 697-705
- [17] del Campo D, Chimenti V, Reyes J, Rodriguez Castillon J A, Moldovan M, Garcia Alonso J I 2008 Assembly and Study of Different Mercury Cells with Known Impurity Content and Isotopic Composition, *Int. J. Thermophys.* **29**, 93-103
- [18] Evans J P, Wood S D 1971 An Intercomparison of High Temperature Platinum Resistance Thermometers and Standard Thermocouples, *Metrologia* **7**, 108-130
- [19] Fahr M, Rudtsch S 2008 A New Method for the Quantification and Correction of Thermal Effects on the Realization of Thermal Effects, *Int. J. Thermophys.* **29**, 126-138
- [20] Furukawa G T 1974 Investigation of Freezing Temperatures of National Bureau of Standards Aluminium Standards, *J. Research Natl. Bur. Stand.* **78A**, 477-495
- [21] Furukawa G T 1992 Realization of the mercury triple point, Temperature, Its Measurement and Control in Science and Industry *American Institute of Physics* (New York) **6**, 281-285
- [22] Gam K S, Kang K H, Kim Y-G 2004 Investigation of New Mercury Triple-point Cells and Dry Cooler Made of Thermoelectric Modules, Proc. 9th International Symposium on Temperature and Thermal Measurements in Industry and Science (TEMPMEKO 2004), 22-25 June 2004, pp. 307-312
- [23] Hermier Y, Bonnier G 1992 The mercury point realization: estimate of some uncertainties, Temperature, Its Measurement and Control in Science and Industry *American Institute of Physics* (New York) **6**, 287-291
- [24] Hill K D 1994 An Apparatus for Realizing the Triple Point of Mercury, *Metrologia* **31**, 39-43
- [25] Ivanova A G, Abasov M Y, Gerasimov S F, Pokhodun A I 2013 Measurement of the In Freezing-Point Temperature: Effect of the Liquid-Solid Interface Structure, AIP Conf. Proc. **1552**, p. 243
- [26] Ivanova A G, Pokhodun A I 1992 Realization of the Freezing Point of Indium, Temperature, Its Measurement and Control in Science and Industry *American Institute of Physics* (New York) **6**, 323-326
- [27] Kalemci M, Ince A T, Bonnier G 2009 Realization of New Mercury Triple Point Cells at TUBITAK UME, XIX IMEKO World Congress Fundamental and Applied Metrology Proc., pp. 1505-1508
- [28] Kalemci M, Ince A T, Bonnier G 2011 Assessment of Methods for Determining the Impurity Concentration in Mercury Cells, *Int. J. Thermophys.* **32**, 269-277
- [29] Large M J, Pearce J V 2014 A Phase-Field Solidification Model of Almost Pure ITS-90 Fixed Points, *Int. J. Thermophys.* **35**, 1109-1126
- [30] Li X, Zhao M, Chen D 2004 Realization of the Freezing Points of Indium, Tin and Zinc Using Stainless Steel-Cased Cells, Proc. 9th International Symposium on Temperature and Thermal Measurements in Industry and Science TEMPMEKO 2004, 22-25 June 2004, pp. 221-226

- [31] Mangum B W 1982, Triple Point of Gallium as a Temperature Fixed Point, Temperature, Its Measurement and Control in Science and Industry *American Institute of Physics* (New York) **5**, 299-309
- [32] Mangum B W 1989, Determination of the indium freezing point and triple point temperatures, *Metrologia* **26**, 211-218
- [33] Mangum B W, Thornton D D 1979 Determination of the Triple-Point Temperature of Gallium, *Metrologia* **15**, 201-215
- [34] Marcarino P, Dematteis R, Fernicola V, Chattle M V, De Groot M, Wessel I, Thrane M, Thrane H, Chimenti V, Pérez J, Liebana G, Côté-Real Filipe M E, Renaot E, Elgourdou M, Bonnier G 1992 An interlaboratory comparison of tin and zinc fixed points, in Temperature: Its Measurement and Control in Science and Industry, vol. **6**, *American Institute of Physics* (New York) pp. 333-338
- [35] Marcarino P, Steur P P M, Dematteis R 2003 Realization at IMGC of the ITS-90 Fixed Points from the Argon Triple Point Upwards, in Temperature: Its Measurement and Control in Science and Industry, vol. **7**, *American Institute of Physics* (New York), pp. 65-70
- [36] McAllan J V, Ammar M M 1972 Comparison of the Freezing Points of Aluminium and Antimony, Temperature: Its Measurement and Control in Science and Industry, vol. **4**, *Instrument Society of America* (Pittsburgh) pp. 275-285
- [37] McLaren E H 1957 The Freezing Points of High Purity Metals and Precision Temperature Standards, *Can. J. Phys.* **35**, 1086-1106
- [38] McLaren E H 1958 The Freezing Points of High Purity Metals as Precision Standards, *Can. J. Phys.* **36**, 585-598
- [39] McLaren E H 1959 Intercomparison of 11 Resistance Thermometers at the Ice, Steam, Tin, Cadmium, and Zinc Points, *Can. J. Phys.* **37**, 422-432
- [40] McLaren E H 1962 The Freezing Points of High-Purity Metals as Precision Temperature Standards, Temperature, Its Measurement and Control in Science and Industry, vol. **3**, (Reinhold, New York) pp. 185-198
- [41] McLaren E H, Murdock E G 1960, The Freezing Points of High Purity Metals as Precision Temperature Standards, *Can. J. Phys.* **38**
- [42] McLaren E H, Murdock E G 1966a Radiation effects in precision resistance thermometry: I. Radiation losses in transparent thermometer sheaths, *Can. J. Phys.* **44**, 2631-2652
- [43] McLaren E H, Murdock E G 1966b, Radiation effects in precision resistance thermometry: II. Illumination effect on temperature measurement in water triple-point cells packed in crushed ice, *Can. J. Phys.* **44**, 2653-2659
- [44] McLaren E H, Murdock E G 1979, *The Properties of Pt-PtRh Thermocouples for Thermometry in the Range 0–1100°C*, Parts I and II, NRC Reports NRCC 17407 and NRCC 17408
- [45] Nakano T, Tamura O, Sakurai H 2008 Realization of the Gallium Triple Point at NMIJ/AIST, *Int. J. Thermophys.* **29**, 112-118

- [46] Neuer G, Brost O 1975, Heat pipes for the realization of isothermal conditions as temperature reference sources, *Temperature Measurement 1975*, Inst. Phys. Conf. Series No 26 (The Institute of Physics, London and Bristol) pp. 446-452
- [47] Nubbemeyer H G 1990, High temperature platinum resistance thermometers and fixed point cells for the realization of ITS-90 (Private Communication)
- [48] Oleinik B N, Ivanova A G, Drinianinov M M, Zamkovets V A 1984 Realization of the indium freezing point, Comité Consultatif de Thermométrie, 15^e Session, Doc. CCT/84-1
- [49] Pavese F, Marcarino P, Giraudi D, Dematteis R 1999 IMGC Cells for the Realization of the Triple Point of Mercury, Proc. 7th International Symposium on Temperature and Thermal Measurements in Industry and Science (TEMPMEKO '99), pp. 112-117
- [50] Pearce J V, Veltcheva R I, Lowe D H, Malik Z, Hunt J D 2012 Optimization of SPRT measurements of freezing in a zinc fixed-point cell, *Metrologia* **49**, 359-367
- [51] Pearce J V, Veltcheva R I, Large M J 2013 Impurity and Thermal Modelling of SPRT Fixed-points, AIP Conf. Proc. **1552**, pp. 283-288
- [52] Petchpong P, Head D I 2007 Argon pressure is maintained in an aluminium thermometric fixed-point cell, *Metrologia* **44**, L73-L75
- [53] Quinn T J 1990 *Temperature*, 2nd edition, Academic Press (London), p. 495
- [54] Ranostaj J, Duris S, Knorova R, Kaskoto M, Vyskocilova I 2011 New SMU Gallium Fixed-Point Cells, *Int. J. Thermophys.* **32**, 1535-1543
- [55] Renaot E, Elgourdou M, Bonnier G 1999 Does the Value of the ITS-90 Temperature Fixed Points Depend on the Thermal Conditions?, Proc. 7th International Symposium on Temperature and Thermal Measurements in Industry and Science (TEMPMEKO '99) pp. 118-123
- [56] Renaot E 2008 Pollution of aluminium ingot during melting-freezing transitions, Comité Consultatif de Thermométrie, 25^e Session, Doc. CCT/08-10 [http://www.bipm.org/cc/CCT/Allowed/24/D10/CCT_Impurity_AI_\(3\).pdf](http://www.bipm.org/cc/CCT/Allowed/24/D10/CCT_Impurity_AI_(3).pdf)
- [57] Renaot E, Martin C 2009 Impact of the time spent in the liquid phase on the liquid-solid transition, Project EUROMET 732 Workshop, Madrid
- [58] Rudtsch S, Fahr M 2008, Improved Characterisation and Certification Procedure for Fixed-Point Cells, *Acta Metrologica Sinica*, **29** (5A), pp. 82-85
- [59] Rudtsch S, Aulich A, Monte C 2013, Stray Thermal Influences in Zinc Fixed-Point Cells, *Temperature: Its Measurement and Control in Science and Industry*, vol. **8**, *American Institute of Physics* (New York) pp. 265-270
- [60] Sawada S 1982 Realization of the triple point of indium in a sealed glass cell, *Temperature, Its Measurement and Control in Science and Industry*, vol. **5**, *American Institute of Physics* (New York) pp. 343-346
- [61] Shulgat O S, Abasov M Y, Fuksov V M, Pokhodun A I 2013 Effect of Heat Removal Along the Rod on Uniformity of the Inner Interface Thickness During the

- Crystallization Initiation, Temperature: Its Measurement and Control in Science and Industry, vol. **8**, *American Institute of Physics* (New York) pp. 295-299
- [62] da Silva R, Teixeira R N 2013 Construction of an Open Tin Cell at INMETRO, Temperature: Its Measurement and Control in Science and Industry, vol. **8**, *American Institute of Physics* (New York) pp. 249-254
- [63] Sostman H E 1977 Melting Point of Gallium as a Temperature Calibration Standard, *Rev. Sci. Instr.* **48**, 127-129
- [64] Steele A G, Hill K D 2002 Investigating the mercury triple point at the National Research Council of Canada, Proc. 8th International Symposium on Temperature and Thermal Measurements in Industry and Science (TEMPMEKO 2001), 19-21 June 2001, pp. 447-452
- [65] Steur P P M and R. Dematteis 2008, The use of bushings with triple point of water cells:
- [66] towards breaking the 50 μ K barrier, *Metrologia* **45**, 529-533 (2008)
- [67] Steur P P M, Dematteis R 2011a Some Curious Results with a Gallium Fixed-Point Cell, *Int. J. Thermophys.* **32**, 285-292
- [68] Steur P P M, Dematteis R 2011b Production of a New Tin Cell at INRIM, *Int. J. Thermophys.* **32**, 303-308
- [69] Strouse G F 1992 NIST Implementation and realization of the ITS-90 over the range 83K to 1235K: Reproducibility, stability, and uncertainties, in Temperature: Its Measurement and Control in Science and Industry, vol. **6**, *American Institute of Physics* (New York) pp. 169-174
- [70] Strouse G 1999 NIST Realization of the Gallium Triple Point, Proc. 7th International Symposium on Temperature and Thermal Measurements in Industry and Science (TEMPMEKO '99), pp. 147-152
- [71] Strouse G 2004 NIST Certification of ITS-90 Fixed-Point Cells from 83.8058 to 1234.93K: Methods and Uncertainties, Proc. 9th International Symposium on Temperature and Thermal Measurements in Industry and Science TEMPMEKO 2004, 22-25 June 2004, pp. 879-884
- [72] Strouse G 2008 *Standard Platinum Resistance Thermometer Calibrations from the Ar TP to the Ag FP*, NIST Special Publication 250-81
- [73] Strouse G, Furukawa G T 1999 Thermal Characteristics of the NIST Fixed-Point Cells, Furnaces, and Maintenance Baths Over the Temperature Range from 83.8058K to 1234.93K, Proc. 7th International Symposium on Temperature and Thermal Measurements in Industry and Science (TEMPMEKO '99), pp. 153-158
- [74] Strouse G F, Lippiatt J 2001 New NIST Mercury Triple-Point Cells, Proc. 8th International Symposium on Temperature and Thermal Measurements in Industry and Science (TEMPMEKO 2001), 19-21 June 2001, pp. 453-458
- [75] Takiya M 1978 Mesure Précise du Point de Congélation de l'Argent avec un Thermomètre à Résistance de Platine, CCT, 12^e Session, Annexe T30, T154-T159

- [76] White D R, Mason R S 2011 Improved Initiation Technique for the Metal Fixed Points, *Int. J. Thermophys.* **32**, 348-359
- [77] Widiatmo J V, Harada K, Yamazawa K, Arai M 2006 Estimation of impurity effect in aluminium fixed-point cells based on thermal analysis, *Metrologia* **43**, 561-572
- [78] Widiatmo J V, Harada K, Yamazawa K, Arai M 2008 Impurity Effect in Silver-Point Realization, *Int. J. Thermophys.* **29**, 158-170
- [79] Widiatmo J V, Harada K, Yamazawa K, Tamba J, Arai M 2011a Confirming Impurity Effect in Silver-Point Realization from Cell-to-Cell Comparisons, *Int. J. Thermophys.* **32**, 2281-2294
- [80] Widiatmo J V, Sakai M, Satou K, Yamazawa K, Tamba J 2011b, M. Arai, Study on the Realization of Zinc Point and Zinc-Point Cell Comparison, *Int. J. Thermophys.* **32**, 309-325
- [81] Yamazawa K, Widiatmo, J V, Arai M 2007 Thermal Analysis of the Heater-Induced Realization of the Tin Fixed Point, *Int. J. Thermophys.* **28**, 1941-1956
- [82] Yan X K, Duan Y N, Ma C F, Lv Z F 2011 Construction of Sodium Heat-Pipe Furnaces and the Isothermal Characteristics of the Furnaces, *Int. J. Thermophys.* **32**, 494-504
- [83] Zhang J T, Wang Y N 2008 Mechanism to Diminish the Supercooling of the Tin Freezing Point by using Graphite Powder, *Int. J. Thermophys.* **29**, 844-851